Velocity Enhancement by Synchronization of Magnetic Domain Walls

Aleš Hrabec,[1] Viola Křižáková,[2] Stefania Pizzini,[2] João Sampaio,[1] André Thiaville,[1] Stanislas Rohart,[1,*] and Jan Vogel[2,†]
[1]*Laboratoire de Physique des Solides, CNRS, Université Paris-Sud, Université Paris-Saclay, 91405 Orsay Cedex, France*
[2]*Université Grenoble Alpes, CNRS, Institut Néel, F-38000 Grenoble, France*

(Received 13 February 2018; revised manuscript received 4 April 2018; published 30 May 2018)

Magnetic domain walls are objects whose dynamics is inseparably connected to their structure. In this Letter, we investigate magnetic bilayers, which are engineered such that a coupled pair of domain walls, one in each layer, is stabilized by a cooperation of Dzyaloshinskii-Moriya interaction and flux-closing mechanism. The dipolar field mediating the interaction between the two domain walls links not only their position but also their structure. We show that this link has a direct impact on their magnetic-field-induced dynamics. We demonstrate that in such a system the coupling leads to an increased domain wall velocity with respect to single domain walls. Since the domain wall dynamics is observed in a precessional regime, the dynamics involves the synchronization between the two walls to preserve the flux closure during motion. Properties of these coupled oscillating walls can be tuned by an additional in-plane magnetic field enabling a rich variety of states, from perfect synchronization to complete detuning.

DOI: 10.1103/PhysRevLett.120.227204

When several similar oscillators are coupled by a weak force, they can adjust their rhythms thanks to entrainment, similar to the original observations of pendulum clocks by Huygens [1]. The field of synchronization covers a vast amount of phenomena in daily life, nature, music, communication, or engineering [2]. In spintronics, spin-torque nano-oscillators have demonstrated a great ability for synchronization via coupling through an electric current, spin waves, or dipolar field [3–6] leading to a narrower linewidth and an increased emitted power. Here we use the physics of synchronization to enhance the velocities of magnetic domain walls (DWs) in thin magnetic bilayers. The interaction between two oscillators, represented by a pair of chiral DWs, is mediated by a dipolar field, which not only links the wall position but also locks their internal structure. The present Letter represents a first experimental realization of a coupled system whose motion can benefit from synchronization [7].

Magnetic DW dynamics usually focuses on velocity response to a driving force (magnetic field or electrical current). However, a DW is not a simple interface described only by its position q, as dynamics is directly connected to its internal structure. In a minimal model [8], q is connected to the angle φ, which describes the DW internal magnetization orientation, and they form a set of conjugated coordinates (Fig. 1). At small driving forces, the motion is steady state and φ adopts a finite value, but above a threshold called Walker breakdown, the DW is no longer able to hold its structure: φ precesses and the velocity drops down [8,9]. In such a regime, the DW behaves as an oscillator as well as a moving interface with a direct link between them. The boundary between the two regimes, set by the DW internal energy, can be efficiently controlled in ultrathin magnetic films by inducing chirality through the Dzyaloshinskii-Moriya interaction (DMI) [10–13]. This unavoidably also changes the DW oscillation properties, such as the precession frequency.

DWs in magnetic multilayers can be coupled via direct exchange across a spacer layer [14–16] or through dipolar fields [17–19]. The benefits of the oscillatory motion have been overlooked so far since the dynamics of these bound DWs was probed in a steady-state regime. In this Letter, we show that a pair of dipolarly coupled DWs moving above the Walker breakdown can synchronize their precession, resulting in a velocity increase. While the DWs are moved by a perpendicular magnetic field, an additional in-plane field allows tuning the oscillator properties to optimize the synchronization and maximize the velocity. This allows exploring a rich variety of synchronized states, from entrainment to complete detuning.

We study a magnetic multilayer [20] of Pt(5)/Co(1.1)/Au(3)/Co(1.1)/Pt(5) (thicknesses in nanometer) with perpendicular magnetic anisotropy where the Au spacer thickness is adjusted in order to ensure purely dipolar coupling between the magnetic layers [19,22]. Such a structure offers a way to constructively combine two chiral interactions [19]: the DMI, whose sign is set by the interface nature [23], and the dipolar fields [17], whose sense is not adjustable. Through the DMI, the Pt/Co interface serves as a source of left- and right-handed chirality [24,25] in the DWs in the bottom and top Co layers, respectively. Therefore, the DWs have opposite chiralities and can be coupled through the stray field in a flux closure manner, illustrated in Fig. 1(a) [19]. To study magnetic-field-induced DW motion, the films were patterned into 10 μm wide stripes using UV lithography and e-beam etching through an aluminium mask.

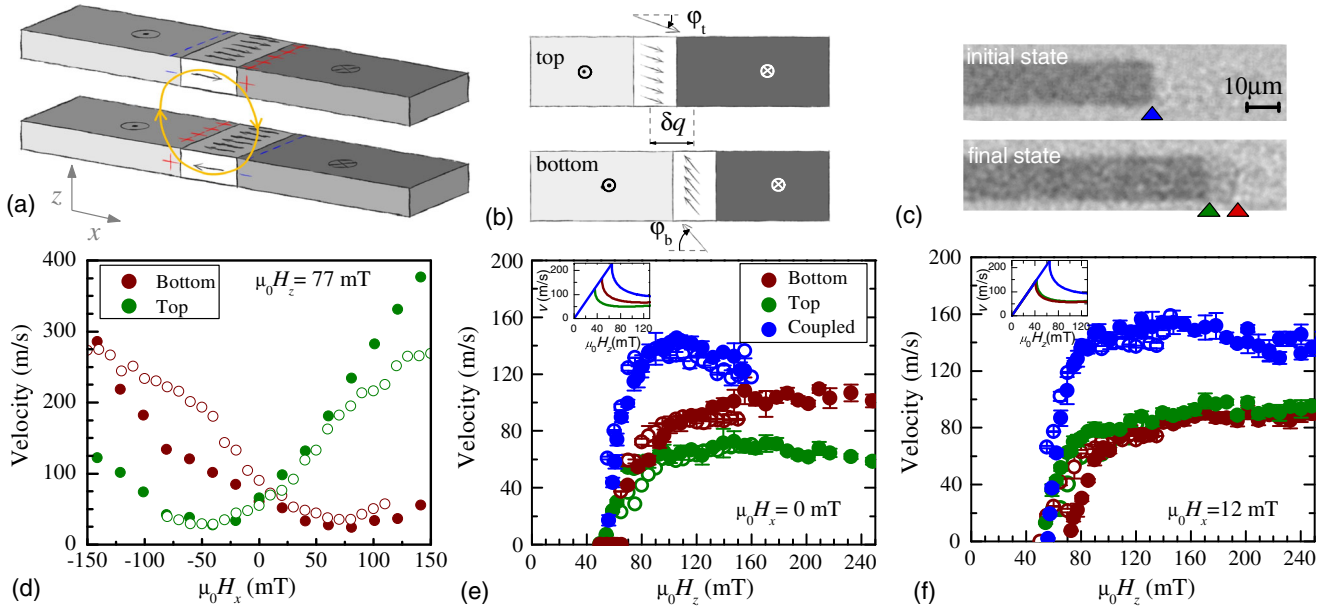

FIG. 1. Coupled domain walls dynamics. (a) Magnetic bilayer track containing two up-down chiral Néel walls coupled by a dipolar field. (b) When an out-of plane field B_z is applied, the top and bottom DW magnetization angles (seen separately in the top view) tilt. DWs are described by magnetization angles φ_b and φ_t inside the bottom and top walls and by their relative position δq. (c) Kerr micrographs in the initial state [coupled DW (blue triangle)] and after application of seven 30-ns-long 150-mT field pulses (bottom), which result in decoupled DWs (green, top layer; red, bottom layer). Dark, light gray, and gray contrasts inside the stripe correspond to $\uparrow\uparrow$, $\uparrow\downarrow$, and $\downarrow\downarrow$ magnetization directions, respectively. (d) Single DW velocity at $\mu_0 H_z = 77$ mT for an up-down DW, as a function of an in-plane field. (e),(f) DW velocity as a function of an out-of-plane field at $\mu_0 H_x = 0$ mT (e) and $+12$ mT (f). In (d)–(f), the color code is the same; full and empty symbols correspond to the experiments and 2D micromagnetic simulations, respectively. Insets in (e),(f) show the calculated curves by the minimal model [8], using the coupled DWs effective DMI constant (strong coupling approximation).

We first focus on the coupled DWs velocity. Polar Kerr magneto-optical microscopy was used to image the DW motion along the wires in response to sequences of 30-ns magnetic field pulses, obtained using a microcoil embedded in a silicon substrate [26]. Coupled DWs were obtained by domain nucleation on natural sample defects, after the application of a 30-ns-long 120-mT field pulse. Different shades of magnetic contrast reveal whether coupled or single DWs are present, as shown in Fig. 1(c) prior and after application of 150-mT pulses leading to DW decoupling. This allows investigating the individual DW behavior and thus the properties of each magnetic layer. Figure 1(e) reveals that the coupled DWs velocity increases up to ≈140 m/s at 100 mT and then gradually decreases until ≈150 mT, where the walls decouple and no longer travel together. The single DW velocity curves are globally similar to that of coupled DWs, but the maximum velocity is significantly lower. Additionally, the DW velocity versus an in-plane field aligned along the wires and driven by $\mu_0 H_z = 77$ mT was measured to evidence the opposite chirality of single walls in each layer [see Fig. 1(d)] [27]. Beyond the DMI sign change, the difference between single wall velocity curves indicates that the magnetic layers are slightly different.

The velocity curves reveal three distinct regimes: a negligible velocity up to 50 mT due to sample defect-induced pinning, a fast velocity increase during a depinning transition (50–70 mT), and a regime where the velocity saturates. The steady-state regime is hindered by defects as the Walker field [see the inset of Fig. 1(e)] is close to the depinning transition [28]. The velocity saturation is typical for precessional dynamics, where the oscillations are perturbed by vertical Bloch lines (VBLs) propagating along the wall [29], and is correlated with the DMI [26,30]. The larger coupled DWs saturation velocity seen in Fig. 1(e) is a direct consequence of the chiral energy increase due to the flux closure.

Micromagnetic simulations [31], including magnetic disorder [32], were used to determine the sample parameters (DMI coefficients D, disorder amplitude and damping parameter α) by finding the best agreement with experiments [see Figs. 1(d)–1(f) and Supplemental Material [20]]. This yields $\alpha = 0.3$, Co thickness fluctuations of 8% and $D_b = -0.73$ mJ/m^2 and $D_t = 0.50$ mJ/m^2 in the bottom and top layer, respectively, manifesting a change of interface quality along the growth direction. These parameters are used to calculate the coupled DWs dynamics [Fig. 1(e)] without further adjusting any of the parameters.

The coupling between DWs is mostly mediated by the stray field arising from the domains and can be decomposed into two components. The stray field acting on the domains generates an attractive spring force between the DWs. The stray field acting on the DW magnetization modifies the DW

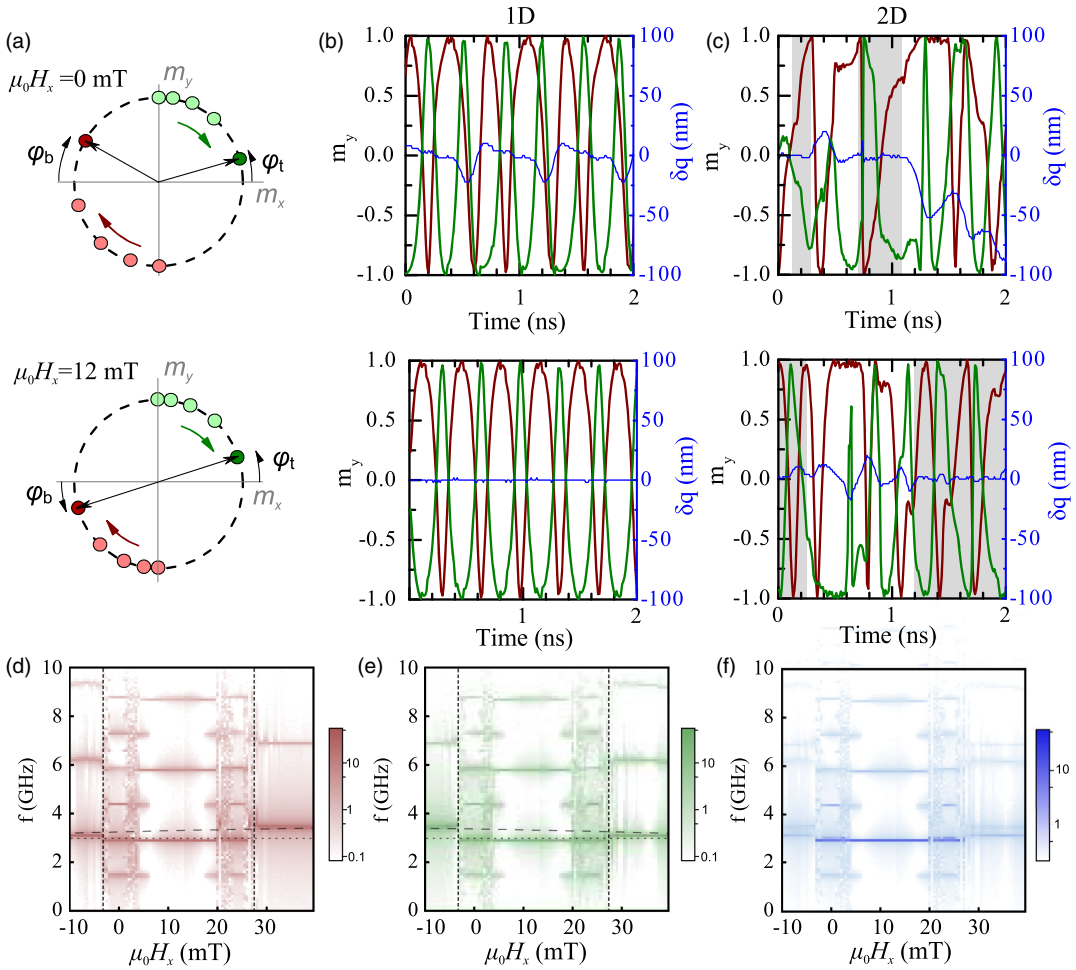

FIG. 2. Simulations illustrating the DW oscillation synchronization. (a) Sketch of the magnetization angle in the center of the bottom (φ_b) and top (φ_t) DWs. In the absence of the in-plane field (top), the two oscillations are detuned, while the appropriate in-plane field (bottom) ensures their locking. (b) Time evolution of m_y for a 1D wire containing a pair of up-down DWs at $\mu_0 H_z = 125$ mT, for $\mu_0 H_x = 0$ mT (top) and +12 mT (bottom). The coupled DW velocity is 98 m/s [inset of Fig. 1(e)]. Green and red curves represent the top and bottom DWs, respectively. The blue curves denote the relative distance between the walls. (c) Evolution of m_y at $\mu_0 H_z = 125$ mT for a 2D system in the middle of the stripe as indicated by the dashed line in Fig. 3(b). (d) Power spectral density of m_y calculated from 1D model (b) for a 20-ns time window, as a function of the in-plane field for the bottom (d) and top (e) DWs. Vertical dashed lines show lower and upper bounds of individual (decoupled) DWs. Gray dashed and dotted lines represent the minimal model [8] results for the coupled (using D_{eff}) and single DWs (using D_b and D_t), respectively. (f) Geometric mean of the values presented in (d) and (e), which underlines the synchronization regions.

energy via a magnetic flux closure and has the same symmetry as the DMI [19]. In a strong coupling approximation, with negligible separation δq and antiparallel magnetization of the two DWs, the coupled DWs can be represented by a single DW with an effective DMI $D_{\text{eff}} = 1.08\ \text{mJ/m}^2$ (73% larger than the average of the DMI coefficients), estimated from static calculations [20]. Hence, the increased Walker field and velocities shown in the inset of Figs. 1(d) and 1(e) are in qualitative agreement with experimental data. Note that the increase scales with the layer magnetization and spacer thickness.

Since the DMI is not equivalent in the two layers, an in-plane field can be used to tune and symmetrize the system by reducing (reinforcing) the stability of the bottom (top) DW [20]. With $\mu_0 H_x = +12$ mT applied in addition to the out-of-plane field, the isolated up-down DW velocities [Fig. 1(f)] approach each other (down-up DWs require an opposite in-plane field sign, but we focus on up-down DWs without any loss of generality). Interestingly, coupled DWs in the symmetrized system display an unchanged maximum velocity, but are more robust, since they do not decouple up to ≈250 mT, while maintaining a constant velocity.

When an out-of-plane field is applied, the magnetization directions φ_b and φ_t inside the bottom and top DWs change proportionally to the field amplitude and, at the Walker breakdown, the DWs turn into chiral Bloch walls ($\varphi_b = \varphi_t = -\pi/2$). However, since experimentally the depinning field is higher than the Walker field, φ_b and

φ_t cannot be stationary. Therefore, maintaining the velocity enhancement requires that the DW coupling remains valid even in such a situation, implying that $\varphi_b = \varphi_t$.

We first start with 1D modeling of the dynamics at $\mu_0 H_z = 125$ mT, for which the DW magnetization undergoes regular precession [Fig. 2(a)]: when the two DWs maintain $\varphi_b = \varphi_t$, they move *together* and *fast*, contrary to the case when the DWs do not lock and lose the benefits of the flux closure. The dynamics is illustrated by 1D micromagnetic simulations [33] [Fig. 2(b)]. Under a 12-mT in-plane field, the two DWs have similar precession frequencies and can lock-in, since the DMI difference is compensated by the in-plane field [20], with $\delta q \approx 0$. As a consequence, the coupled DW velocity is larger than the single DWs (98 m/s as compared to 57 m/s). For a detuned system [see Fig. 2(b) with no in-plane field], the single DW precession frequency difference makes synchronization more complex: the relationship $\varphi_b = \varphi_t$ is not perfectly fulfilled and results in δq oscillations. For even larger detuning, synchronization becomes impossible and the walls separate.

To explore synchronization in more detail, we have computed m_y spectral densities as a function of the in-plane field [Figs. 2(d) and 2(e)] for each DW. The DWs are only coupled for $-3 < \mu_0 H_x < +27$ mT. Outside of this interval, the DWs are spatially separated and their magnetizations oscillate at their natural frequencies estimated by the minimal model [8] (gray dashed lines). The geometrical average of these spectral densities [Fig. 2(f)] emphasizes the synchronization. The simplest synchronized state is found for $+6 < \mu_0 H_x < +18$ mT, which is centered around the perfectly tuned situation. It displays a ground precession frequency f_0 of 3 GHz at $\mu_0 H_z = 125$ mT, corresponding to the precession of a single DW with the effective DMI (gray dotted lines). This range is surrounded by zones of more complex synchronization with the appearance of $f_0/2$ frequencies, frequency emission over a continuous frequency range, and suggests more a chaotic relationship [20].

The situation in a real medium, with 2D degrees of freedom, is more complex since the DW oscillations are perturbed by VBLs and structural disorder. In Fig. 3(b) are displayed snapshots of the DW motion under $\mu_0 H_z = 125$ mT for three different in-plane fields (see also in the Supplemental Material Videos [34]). For a +12-mT in-plane field, the DWs mostly overlap with small separation fluctuations [Fig. 3(a)], which underlines the strong coupling efficiency. For a slightly detuned system (here at zero in-plane field), a larger separation is observed, together with a velocity decrease [inset of Fig. 3(a)]. Ultimately, at even larger detuning (for $\mu_0 H_x \leq -5$ mT, similar to the 1D model), the two DWs are not able to hold together and their separation gradually increases until they decouple and move independently.

To locally probe the magnetization variation correlation, i.e. the local DW coupling, the time evolution of magnetization at the center of the DW [the line cut indicated in Fig. 3(b)] is shown in Fig. 2(c) for $\mu_0 H_x = +12$ and 0 mT (without any structural disorder for simplicity). Even with the symmetrizing field, synchronization is not always observed, but time intervals of synchronization are more frequent and longer than in the detuned system. During the nonsynchronized intervals, DWs are misaligned since the coupling is lost (and vice versa). However, synchronization can be recovered in this 2D situation, since, at a given time, some portions along the DWs are still coupled, as observed in the Supplemental Material Videos [34]. These parts drag and accelerate the rest of the DW pair and the DWs decouple once the synchronized sections are no longer able to drag the separated DWs with lower mobilities.

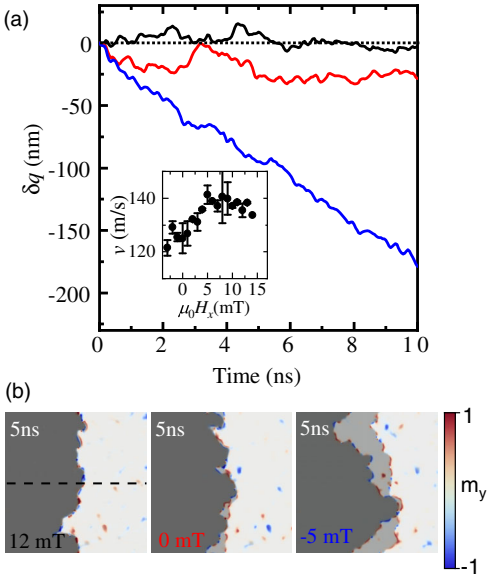

FIG. 3. Simulation of DW motion in a 2D disordered medium. (a) Calculated evolution of the average distance between bottom and top DWs at $\mu_0 H_z = 125$ mT for $\mu_0 H_x = +12$ (black), 0 mT (red), and −5 mT (blue). The inset shows the resulting coupled DWs velocities as a function of the in-plane field. (b) Snapshots of the two DWs dynamics at 5 ns, corresponding to (a). The dark gray contrast corresponds to the ↑↑ state, light gray to the ↑↓ state, and white contrast to the ↓↓ state. The m_y component is reflected by the red ($m_y = 1$) and blue ($m_y = -1$) color scheme. The size of the moving box centered on the top wall is 1×1 μm^2.

To summarize, we have experimentally shown that the dipolar coupling of magnetic domain walls in superposed layers leads to a large velocity increase. This phenomenon is robust against domain wall magnetization precession and disorder. At first sight, especially when DWs have different properties, this is unexpected and implies that the wall magnetization dynamics synchronizes. Systems where the motion of coupled oscillators can benefit from their synchronization have been recently theoretically described as "swarmalators" [7]. The study here can be seen as an experimental realization of such a system, with two swarming objects.

We thank Joo-Von Kim, Julie Grollier for fruitful discussions, and Jacques Miltat for critical comments on the manuscript. This work has been supported by the Agence Nationale de la Recherche (France) under Contracts No. ANR-14-CE26-0012 (Ultrasky), No. ANR-17-CE24-0025 (TopSky), No. ANR-09-NANO-002 (Hyfont), and the RTRA Triangle de la Physique (Multivap).

A. H. and V. K. contributed equally to this work.

*stanislas.rohart@u-psud.fr
†jan.vogel@neel.cnrs.fr

[1] C. Huygens, *Oeuvres complètes de Christiaan Huygens* (Martinus Nijhoff, La Haye, 1893).
[2] A. Pikovsky, M. Rosenblum, and J. Kurths, *Synchronization: A Universal Concept in Nonlinear Sciences*, Vol. 12 (Cambridge University Press, Cambridge, England, 2003).
[3] F. Mancoff, N. Rizzo, B. Engel, and S. Tehrani, Nature (London) **437**, 393 (2005).
[4] S. Kaka, M. R. Pufall, W. H. Rippard, T. J. Silva, S. E. Russek, and J. A. Katine, Nature (London) **437**, 389 (2005).
[5] J. Grollier, V. Cros, and A. Fert, Phys. Rev. B **73**, 060409 (2006).
[6] M. R. Pufall, W. H. Rippard, S. E. Russek, S. Kaka, and J. A. Katine, Phys. Rev. Lett. **97**, 087206 (2006).
[7] K. P. O'Keeffe, H. Hong, and S. H. Strogatz, Nat. Commun. **8**, 1504 (2017).
[8] J. Slonczewski, AIP Conf. Proc. **5**, 170 (1972).
[9] M. Hayashi, L. Thomas, C. Rettner, R. Moriya, and S. S. Parkin, Nat. Phys. **3**, 21 (2007).
[10] M. Heide, G. Bihlmayer, and S. Blügel, Phys. Rev. B **78**, 140403 (2008).
[11] A. Thiaville, S. Rohart, E. Jué, V. Cros, and A. Fert, Europhys. Lett. **100**, 57002 (2012).
[12] K.-S. Ryu, L. Thomas, S.-H. Yang, and S. S. P. Parkin, Nat. Nanotechnol. **8**, 527 (2013).
[13] S. Emori, U. Bauer, S.-M. Ahn, E. Martinez, and G. Beach, Nat. Mater. **12**, 611 (2013).
[14] S.-H. Yang, K.-S. Ryu, and S. Parkin, Nat. Nanotechnol. **10**, 221 (2015).
[15] S. Lepadatu, H. Saarikoski, R. Beacham, M. J. Benitez, T. A. Moore, G. Burnell, S. Sugimoto, D. Yesudas, M. C. Wheeler, J. Miguel *et al.*, Sci. Rep. **7**, 1640 (2017).
[16] P. J. Metaxas, R. L. Stamps, J.-P. Jamet, J. Ferré, V. Baltz, B. Rodmacq, and P. Politi, Phys. Rev. Lett. **104**, 237206 (2010).
[17] A. Bellec, S. Rohart, M. Labrune, J. Miltat, and A. Thiaville, Europhys. Lett. **91**, 17009 (2010).
[18] I. Purnama, I. S. Kerk, G. J. Lim, and W. S. Lew, Sci. Rep. **5**, 8754 (2015).
[19] A. Hrabec, J. Sampaio, M. Belmeguenai, I. Gross, R. Weil, S. Chérif, A. Stashkevich, V. Jacques, A. Thiaville, and S. Rohart, Nat. Commun. **8**, 15765 (2017).
[20] See Supplemental Material at http://link.aps.org/supplemental/10.1103/PhysRevLett.120.227204 for additional information about the sample, micromagnetic parameter determination, domain wall energy, domain wall dynamics, and further insights into domain wall synchronization, which includes Ref. [21].
[21] J. Pellegren, D. Lau, and V. Sokalski, Phys. Rev. Lett. **119**, 027203 (2017).
[22] V. Grolier, D. Renard, B. Bartenlian, P. Beauvillain, C. Chappert, C. Dupas, J. Ferré, M. Galtier, E. Kolb, M. Mulloy *et al.*, Phys. Rev. Lett. **71**, 3023 (1993).
[23] A. Belabbes, G. Bihlmayer, F. Bechstedt, S. Blügel, and A. Manchon, Phys. Rev. Lett. **117**, 247202 (2016).
[24] H. Yang, A. Thiaville, S. Rohart, A. Fert, and M. Chshiev, Phys. Rev. Lett. **115**, 267210 (2015).
[25] E. C. Corredor, S. Kuhrau, F. Kloodt-Twesten, R. Frömter, and H. P. Oepen, Phys. Rev. B **96**, 060410 (2017).
[26] T. H. Pham, J. Vogel, J. Sampaio, M. Vaňatka, J.-C. Rojas-Sánchez, M. Bonfim, D. Chaves, F. Choueikani, P. Ohresser, E. Otero *et al.*, Europhys. Lett. **113**, 67001 (2016).
[27] M. Vaňatka, J.-C. Rojas-Sánchez, J. Vogel, M. Bonfim, M. Belmeguenai, Y. Roussigné, A. Stashkevich, A. Thiaville, and S. Pizzini, J. Phys. Condens. Matter **27**, 326002 (2015).
[28] R. D. Pardo, W. S. Torres, A. B. Kolton, S. Bustingorry, and V. Jeudy, Phys. Rev. B **95**, 184434 (2017).
[29] A. Malozemoff and J. Slonczewski, Phys. Rev. Lett. **29**, 952 (1972).
[30] Y. Yoshimura, K.-J. Kim, T. Taniguchi, T. Tono, K. Ueda, R. Hiramatsu, T. Moriyama, K. Yamada, Y. Nakatani, and T. Ono, Nat. Phys. **12**, 157 (2016).
[31] A. Vansteenkiste, J. Leliaert, M. Dvornik, M. Helsen, F. Garcia-Sanchez, and B. Van Waeyenberge, AIP Adv. **4**, 107133 (2014).
[32] I. Gross, W. Akhtar, A. Hrabec, J. Sampaio, L. Martinez, S. Chouaieb, B. Shields, P. Maletinsky, A. Thiaville, S. Rohart *et al.*, Phys. Rev. Mater. **2**, 024406 (2018).
[33] The 1D micromagnetic simulations were performed similarly as 2D simulations using MuMax [31], for 8 μm long, 1 cell wide stripes, using periodic boundary conditions along the stripe width.
[34] Videos in the Supplemental Material at http://link.aps.org/supplemental/10.1103/PhysRevLett.120.227204 show 15-ns-long simulations of the coupled domain wall motion under a 125-mT out-of-plane magnetic field at several in-plane fields. See description in [20].